

Real-time Friendly Representation of Arbitrary BRDF with Appearance Industry Measurements

ROMAN ĐURIKOVIČ and IVAN ŠEDO

Abstract

This work is devoted to the problem of representing bidirectional reflectance distribution function (BRDF) as ordinary function and to representation of precomputed radiance transfer (PRT) data of a static scene. PRT data set is the discretization of light transfer operator and it is the derivative carrier of information about BRDF used. We discuss the need and principles of industrial appearance measurement attributes. Another part of our work is the implementation of the environment mapping using efficient wavelet rotation. This technique allows dynamic change of lighting, viewpoint and BRDF while preserving all-frequency details. Other implemented feature is the virtual glossmeter. As a feedback to the user it provides gloss unit value measured from the used parametrizable BRDF.

Mathematics Subject Classification 2000: I.3.6, I.3.7

Additional Key Words and Phrases: Appearance, gloss, BRDF

1. INTRODUCTION

The appearance of an object is the result of a complex interaction of the light incident on the object, the optical characteristics of the object, and human perception.

Appearance often determines the acceptability of a product to the end-user. The quality and consistency of the appearance of a product is psychologically related to its expected performance and useful life. It therefore determines its acceptance or rejection by potential purchasers.

The three elements of human perception – light, object and observer, can be quantified and further reduced to a set of colorimetric specifications. These colorimetric specifications can be converted into a variety of color and difference scales which can be used for numerical specifications. Various methods of measurement are available including the basic CIE optical geometries for colorimeters and spectrophotometers, gloss meters, gonio-photometers, gonio-spectrophotometers and image analysis.

All those methods require careful attention in selecting the specimen, measurement techniques, instrument calibration, standardization and verification and validation. This will provide means for more objective appearance communication thus minimizing disagreements and product returns. There are active programs to standardize such observations and measurements, in the American Society for Testing and Materials (ASTM) and in a joint BAM and DIN Committee in Germany. Appearance prediction and appearance engineering both rely on accurate physically based models of light interaction.

Metallic and pearlescent colors are rendered using three aspecular measurements defined in a proposed standard for goniochromatic color. Westlund *et al.* [10] try to apply appearance standards (gloss, haze) to light reflection models (Phong, Ward, Cook-Torrance).

Gloss and *haze* are appearance attributes resulting from the first surface reflection. Gloss is an uncomplicated appearance attribute – an object is either glossy or matte. Gloss is a measure of the magnitude of the specular reflection and haze captures the width of the specular lobe.

Metallic paints and plastics have been widely used but relevant scientific concepts and terminology to describe the appearance of these materials has not yet been established and are still evolving. By *metallic* we identify paints and plastics containing metal flake pigments rather than object made of metal which is a common understanding for the term.

The attributes of appearance of these materials are of two kinds, those observed at a distance of several meters and those observed at reading distance. The first kind may be called *macro appearance*, the second *micro appearance*.

Gloss is defined by the American Society for Testing and Materials (ASTM) to be ‘the angular selectivity of reflectance, involving surface-reflected light, responsible for the degree to which reflected highlights or images of objects may be seen as superimposed on a surface’ [2]. We can differentiate several types of gloss measured at specific angles:

Specular gloss. Specular gloss is measured for the exact mirror direction.

Sheen. Sheen measures the shininess at grazing angles.

Luster. Contrast gloss or luster is a relative measure between specular reflecting areas and other areas.

Haze. Bloom and haze describe the milky appearance, adjacent to specular reflections.

DOI. Distinctness-of-image gloss measures the sharpness of mirror images, relevant for high-gloss surfaces.

Diffuseness. In addition to the gloss one may express the diffuseness of a high-gloss surface by a measurement far of the mirror direction.

2. COMPENDIUM ON PRT METHODS

Under assumption that the object is not emissive, it is common to view light transport as a linear operator [9] [7]. The light that arrives to observer eye is a linear transformation of the distant incident lighting.

The light transport operator \mathcal{L} , encodes the effects of the material properties and light transport interactions between different patches of the object. Thus we can describe the exit radiance $B(\vec{x}, \omega_o)$ at a point \vec{x} on the object surface along the outgoing (viewing) directions ω_o as the result of applying out integral operator \mathcal{L} on the (distant) incident lighting L

$$B(\vec{x}, \omega_o) = (\mathcal{L}L)(\vec{x}, \omega_o) = \int_S T_{\vec{x}, \omega_o}(\omega_i) L(\omega_i) d\omega_i$$

where $T_{\vec{x}, \omega_o}$ is the integration kernel of \mathcal{L} , called the *transport function*. For fixed \vec{x} and ω_o , $T_{\vec{x}, \omega_o}$ is a 2D function parametrized over the sphere S of incoming directions. For a given direction ω_i it describes the contribution of $L(\omega_i)$ to the total reflected radiance leaving \vec{x} along ω_o . Substituting for the integration kernel we can derive the familiar reflectance equation for direct lighting.

With

$$T_{\vec{x}, \omega_o} = f_r(\omega_i, \omega_o) V_{\vec{x}}(\omega_i)(\vec{n}_{\vec{x}})$$

where ω_i is the incoming directions $\vec{n}_{\vec{x}}$ is the surface normal at \vec{x} , $V_{\vec{x}}$ is a binary visibility functions, f_r is the bidirectional reflectance distribution functions, we get

$$B(\vec{x}, \omega_o) = \int_{\Omega} f_r(\omega_i, \omega_o) V_{\vec{x}}(\omega_i) (\vec{n}_{\vec{x}}) L(\omega_i) d\omega_i.$$

However, the integration kernel $T_{\vec{x}, \omega_o}$ is not limited to direct illumination, and can describe many other complex transport effects such as interreflections, refraction, self-occlusion, caustics, subsurface scattering, and other indirect lighting.

Unfortunately, direct evaluation of $\mathcal{L}L$ is feasible. Even assuming the distant lighting, light transport is 6D (two dimensions for each, lighting (assumed to be at infinity) and view direction and two dimensions for the surface position) and fundamentally all previous PRT work is concerned with approximating and compressing some slice of the light transport operator.

Precomputed light transport techniques compute a pixel color at render-time based on a precomputed approximation of the light transport operator, which evaluates the contribution of all lighting directions for a given spatial location on a mesh and a given view direction.

The key issue common to all PRT techniques is the representation of the light transport operator. There are several criteria used to judge the quality of any proposed representation: rendered visual quality, compactness, storage costs, efficient integration/evaluation, angular and spatial frequency bandwidth (sharpness) of the illumination effects.

The precomputed radiance (PRT) algorithm [9] has recently attracted much attention owing to its ability to allow real-time rendering of complex objects under dynamic lighting environments.

First PRT methods (SH based) either only handled low-frequency lighting environments, or suffer from the unwieldy size of PRT data sets even after compression. For dynamic scenes, the amount of PRT data sets further expands to an impractical degree for real-time applications. The enormous PRT data sets often prohibit high-quality rendering, subsequently restricting practical application of the PRT algorithm.

Typically, the transport operator is represented by linear basis functions such as spherical harmonics or wavelets, and the number of coefficients directly constrains the sharpness of the effects that can be handled.

The PRT algorithm can capture self-shadowing and self-interreflection effects from dynamic lighting environments. As a preprocess, PRT precomputes a solution to the light transport of a scene, and records the simulation results.

To decrease data storage and computational costs, the recorded data are compressed for efficient rendering at run-time. Low-frequency methods projected the per-vertex light transfer functions onto the spherical harmonics basis [9] [4].

The coherence among vertices was then exploited using principal component analysis or CPCA [8] [4].

By contrast the all-frequency PRT methods [6] [7] [5] approximated the densely-sampled PRT data with sophisticated compression techniques, such as non-linear wavelet approximation [6] [7] [1] and BRDF factorization [1] [5].

However, previous compression schemes are inadequate for harnessing the power of PRT. Based on the SH basis, the low-frequency PRT algorithms may take tens of thousands of terms to represent all-frequency lighting and shadowing effects. As for the all-frequency PRT algorithms, the compressed data are still cumbersome for real-time rendering of ob-

jects with glossy BRDFs.

Ng *et al.* [6] use nonlinear approximation (truncation) of wavelets as basis function instead of spherical harmonics. With as few as 100 coefficients, they are able to incorporate high-frequency lighting effects (for diffuse surfaces or static view only). The significant coefficients are selected based on incident lighting which prevents the use of highly glossy surfaces.

2.1 SH Based Methods

Sloan *et al.* were the first who presented in [9] new real-time method for rendering diffuse and glossy object in low-frequency lighting environments that captures soft shadows, interreflections and caustics.

By representing both incident radiance (lighting) and transfer functions using low-order spherical harmonics linear basis, authors exploit the linearity to reduce the light integral to a simple dot product between corresponding coefficient vectors (diffuse receivers) or a simple linear transform of the lighting coefficient vector through a small transfer matrix (glossy receivers).

3. VIRTUAL LIGHT METER

The measure of a gloss is a simplification of the BRDF to single appearance related attribute. We proposed a virtual light meter for the purpose of correspondence between BRDF model parameters and standard appearance measurements. In fact, it is a customized 2D integration tool which uses numerical quadrature of particular BRDF over subdivided light source and detector apertures, which simulates the work of a real-life light meter. The light source light hits the surface being measured and the detector catches the reflected light and evaluates the numerical result.

Virtual light meter can be used to evaluate known standards such as specular gloss, haze, *etc.* and can be customized for other measurements. In our work we implemented the glossmeter. The measurement of specular gloss consists of comparing the luminous reflectance from tested specimen to that from a gloss standard, under some geometric and spectral conditions well defined by national or international standards *e.g.* ISO 2813 [3].

Those standards usually prescribe the measurements to be taken at angles 20°, 60° and 85° as illustrated at Figure 1, because these degrees of specular gloss measurements offer numerical values which are roughly linearly correlated over a range of values to perceived gloss of high-gloss, medium-gloss, and low-gloss surfaces, respectively. The numerical gloss value, assigned to a surface typically ranges from 0 (low gloss) to 100 (high gloss).

4. VIRTUAL GLOSSMETER

To implement virtual glossmeter we need a 2D integration tool to compute the equation for the total exitant flux $\Phi_{S,D}(\rho)$ passing through the detector aperture for derivation, please, have a look at original paper [10]:

$$\Phi_{S,D}(\rho) = AL_S \sum_{k=1}^K \sum_{j=1}^J \rho(\vec{s}_j, \vec{d}_k) (\vec{s}_j \cdot \vec{n}) d\omega_{S_k} (\vec{d}_k \cdot \vec{n}) d\omega_{D_k},$$

where S_j is the j -th patch of the source aperture, s_j is the unit direction vector of S_j , \vec{n} is the unit normal vector to surface element dA , $d\omega_{S_k}$ is the solid angle subtended by S_k at dA , D_k is the k -th patch of the detector aperture, d_k is the unit direction vector of D_k , $d\omega_{D_k}$

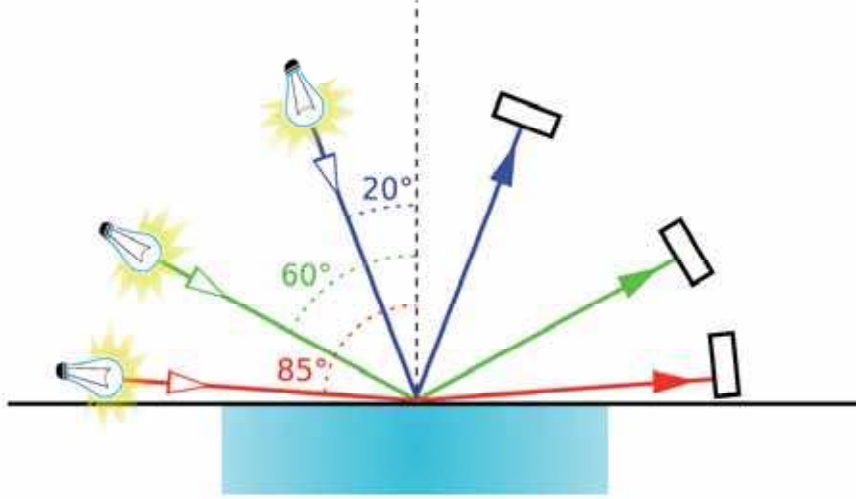


Fig. 1: Glossmeter measurements at various angles.

is the solid angle subtended by D_k at dA . The source radiance, L_S , is constant so this was brought out of the double sum. The BRDF, ρ , is explicitly listed as parameter of Φ to add clarity for when we later compare the exitant flux resulting from different surfaces.

In our work we use the library *Cuba* to compute cubature. We integrate over the rectangle aperture of the detector and then the integration over the rectangle aperture of a light source is performed. Cuba library takes care of adaptive subdivision during the integration.

In order to compute gloss value, we need to compute and compare the total exitant flux of measured surface and total exitant flux of a standard surface and divide them

$$G = 100 \frac{\sum_{k=1}^K \sum_{j=1}^J \rho(\vec{s}_j, \vec{d}_k) d\Omega_{S_j} d\Omega_{D_k}}{\sum_{k=1}^K \sum_{j=1}^J F(\vec{n}, \vec{s}_j) \delta(\text{mirror}(\vec{s}_j) - \vec{d}_k) d\Omega_{S_j}}$$

where F is the Fresnel reflectivity for unpolarized light, n is the refractive index of the standard, and $\text{mirror}(\vec{s}_j)$ is the unit mirror direction vector of \vec{s}_j . $d\Omega_{S_j}$ and $d\Omega_{D_k}$ are the projected solid angles of the source and detector patches, respectively. The mirror direction vector can be computed with:

$$\text{mirror}(\vec{s}_j) = 2(\vec{s}_j \cdot \vec{n})\vec{n} - \vec{s}_j.$$

Delta function is

$$\delta(\vec{v}) = \begin{cases} 1 & \text{if } |\vec{v}| < \epsilon, \\ 0 & \text{if } |\vec{v}| \geq \epsilon. \end{cases}$$

The numerical gloss value, G , is measured in so called *gloss units* (GLU) and typically ranges from 0 (low gloss) to 100 (high gloss). As is expected, the sample area and source radiance drop out of the equation of gloss; specular gloss becomes a function of BRDF, index of refraction and geometry. The evaluation time of our virtual glossmeter takes from fractions of a second to few second, depending on the measurement angle and BRDF parameters.

By definition, the ultimate standard surface for gloss measurements is a smooth black glass surface having a refractive index of 1.567 for the wavelength 589.26 nm for all an-

gles. For all angles of incidence this surface by definition has an assigned gloss value of 100 GLU. The blackness limits the exitant flux to first standard reflection and smoothness ensures presence of reflections only in specular direction. Corresponding specular reflectance values at 20° , 60° and 85° computed using the Fresnel equations are approximately 0.049, 0.998, and 0.619.

5. DATA ACQUISITION

We use two approaches to build up a database of paint and coatings appearance attributes. In our first approach we will utilize industry standard appearance measurement devices, which are used to determine the quality and acceptability of a variety of product finishes. On the other hand, the current industry standards reduce the measurements result only to few samples, which is not enough to reproduce directly any reasonable BRDF by sampling. However our goal is to investigate the possibilities to use these devices as validation tools of our analytic BRDF models for car paints.

We use a standard glossmeter and a colorimeter. The glossmeter conforms the [3] standards and is able to measure gloss and reflectance under the geometry of three angles: 20° , 60° , 85° . The colorimeter measures the tristimulus color of the diffusely lightened surface viewed at 8° from normal direction with a $d/8$ geometry.

6. GPGPU NONSTANDARD HAAR WAVELET TRANSFORM

The need of storing rotation matrices in the memory for all the time was bothering us from the first time. Once the lighting changes it is transformed to local slices induced by normal directions. These slices are then indexed and dotted with BRDF slices in rendering routine. We came with an idea to bypass the transforming the global light to many local slices, by dropping the memory consuming transformation matrices, and sample the wavelet transform slices on the GPU. We usually use the setup of 32×32 normal samples (in octahedral parametrization) and the size of local slice is 32×32 , too. Easy calculation can prove, that if we tiled local slices side by side, row by row, we would end up with tileboard of size 1024×1024 which fits into the GPU memory.

For each slice induced by normal we first sample the HDR lighting in the direction of this normal. Those HDR image data are stored on graphics card until the whole Haar transform is performed and only after that those data are sent to system memory, where there are transformed to sparse vectors as in purely CPU version. Haar transform is performed in the fragment shader by horizontal and vertical steps on all the tiles.

For this we use the well known *ping pong* technique of two image buffers (textures) the first texture is used as a source for the shader. Assuming horizontal step we execute shader with parameters indicating level of the transform (*i.e.* what data to transform and what data to pass unchanged). Next, the roles of the textures are swapped, therefore the second texture serves as input for shader and we run the vertical step, and so on. For better understanding look at Fig. 2.

We encountered slow-down when determining what kind of operation (averaging, difference of pass) has to be performed for a pixel in question by fragment shader. We rather precomputed these conditions and store them in RGB texture as can be seen in Figure 3. This helped us to speed up dynamic change of lighting by factor of 2-3.

Real-time BRDF with Industry Measurements

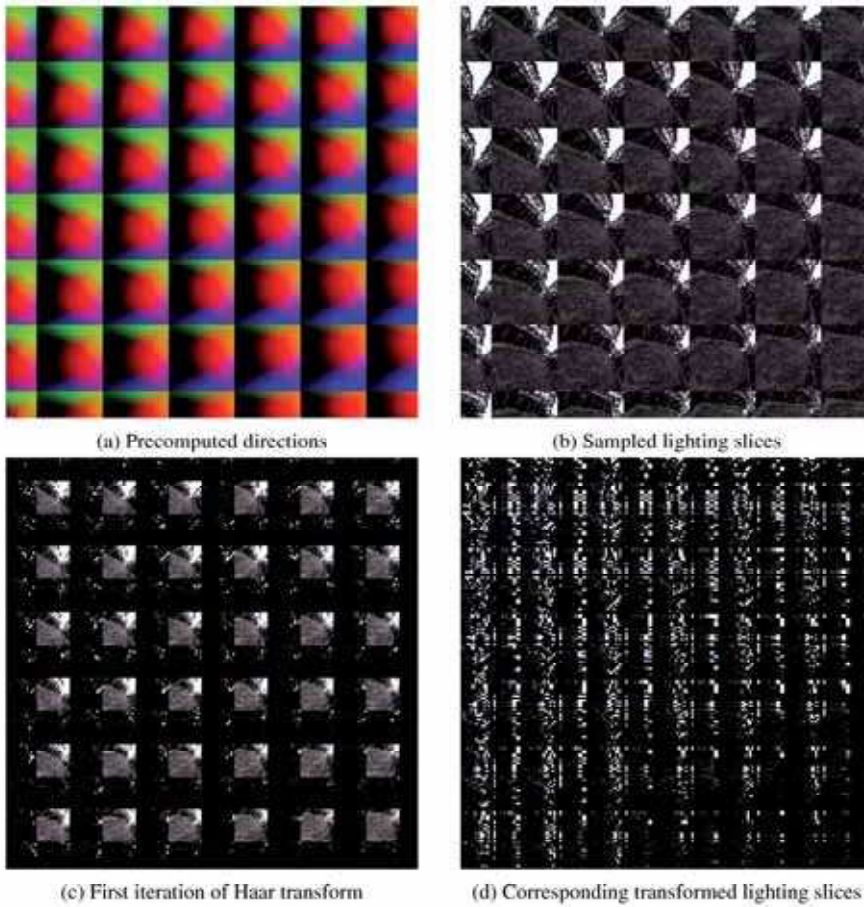


Fig. 2: Visualization of GPU Haar transformation tileboards (cropped)

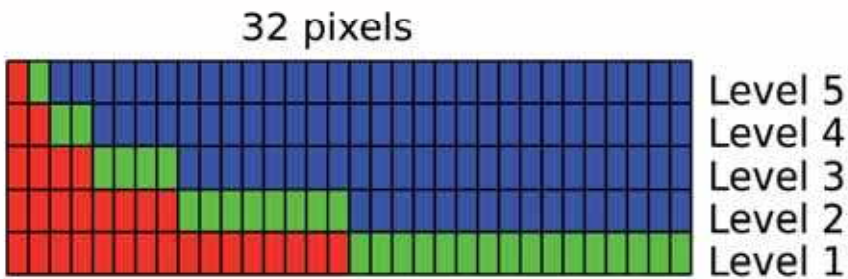


Fig. 3: Domain decomposition for GPU Haar transform (red denotes positions where low-pass filter results are stored, green high-pass and blue identical values)

7. IMPLEMENTATION

Our visualization tool works with projects, which can be saved to and loaded from a file. Each project consists of arbitrary number of HDR lightings and 3D models. Each model



Fig. 4: Example of Cook-Torrance PRT visualization.

may have assigned BRDF along with corresponding parameters, see Fig. 4. Only one lighting and one model can be displayed at a time. Project data file is stored as zlib compressed binary data stream.

Our implementation of virtual glossmeter is fully customizable. User can change size and location of apertures, specular angle and surface orientation. For now we show off few synthetic BRDF setups with corresponding measured gloss unit results in Figure 5.

8. CONCLUSION

We implemented environment mapping visualization tool preserving all frequencies in BRDF and lighting environments. Our contribution to the original work lies in the support of multi-core CPUs, which speeds up the pre-computation and rendering code almost linearly to the number of cores available.

Another contribution is the profit from the presence of fast programmable graphic processor, which we use to perform tile-boarded nonstandard Haar wavelet transform. This is a step toward more dynamic changes of the lighting environment and it also overcomes the need of keeping rotation matrices in the memory, thus lowers the overall consumed memory.

In summary, we implemented stand alone visualization tool enabling us to render highly specular materials under natural detail lighting environments at interactive rates, employing multi-core CPU and fast GPU to speed up computation, while giving the virtually measured numerical specular gloss value of rendered material as feedback to the user.

In the future we would like to extend environment mapping technique to triple product integral scene relighting and thus incorporating soft-shadowing of objects.

Acknowledgments

This research was sponsored by grants from the EU-FP6-MC-040681- APCOCOS.

REFERENCES

- 0003, R. W., TRAN, J., AND LUEBKE, D. P. All-frequency relighting of non-diffuse objects using separable brdf approximation. In *Rendering Techniques* (2004), pp. 345–354.

Real-time BRDF with Industry Measurements

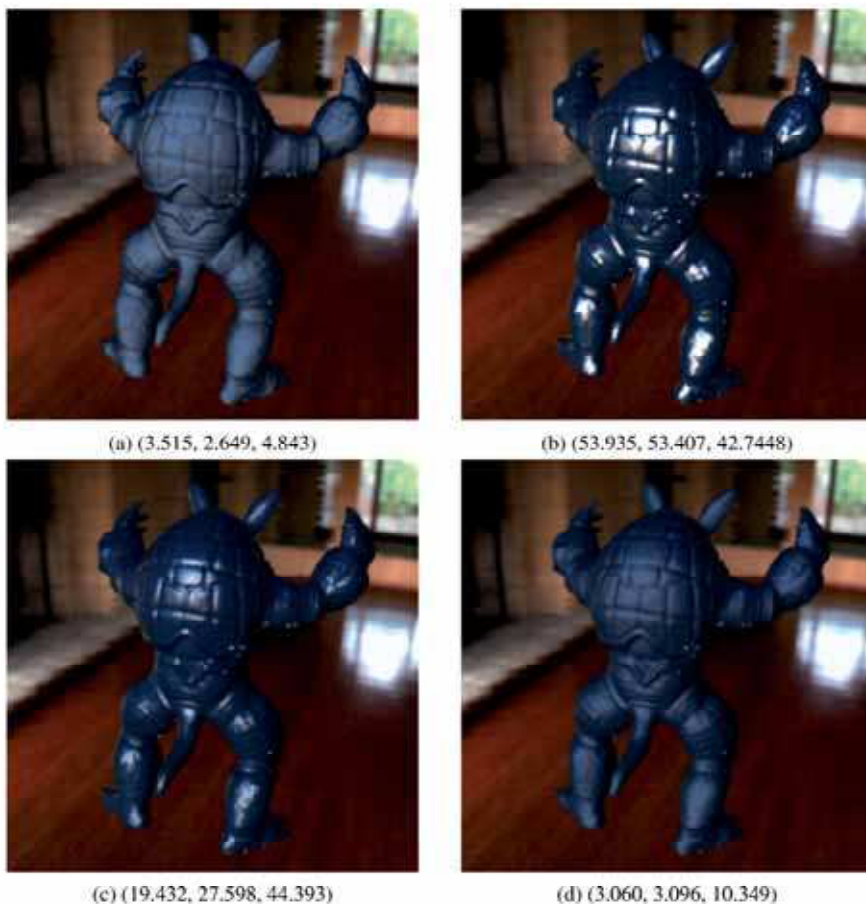


Fig. 5: Example virtual glossmeter measurements at 20°, 60° and 85° angles in gloss units. Scene with Stanford Armadillo model and Ennis lighting environment.

ASTM. *ASTM D 523-89: Standard Test Method for Specular Gloss*. ASTM, 1999.

ISO. *ISO 2813: Paints and varnishes -Determination of specular gloss of non-metallic paint films at 20 degrees, 60 degrees and 85 degrees*. Internation Organization for Standardization, 1994.

LEHTINEN, J., AND KAUTZ, J. Matrix radiance transfer. In *SIGD '03: Proceedings of the 2003 symposium on Interactive 3D graphics* (New York, NY, USA, 2003), ACM Press, pp. 59–64.

LIU, X., SLOAN, P. P., SHUM, H. Y., AND SNYDER, J. All-frequency precomputed radiance transfer for glossy objects. In *Eurographics Symposium on Rendering* (Norrkping, Sweden, 2004), A. Keller and H. W. Jensen, Eds., Eurographics Association, pp. 337–344.

NG, R., RAMAMOORTHY, R., AND HANRAHAN, P. All-frequency shadows using non-linear wavelet lighting approximation. In *SIGGRAPH '03: ACM SIGGRAPH 2003 Papers* (New York, NY, USA, 2003), ACM Press, pp. 376–381.

NG, R., RAMAMOORTHY, R., AND HANRAHAN, P. Triple product wavelet integrals for all-frequency re-lighting. In *SIGGRAPH '04: ACM SIGGRAPH 2004 Papers* (New York, NY, USA, 2004), ACM Press, pp. 477–487.

SLOAN, P.-P., HALL, J., HART, J., AND SNYDER, J. Clustered principal components for precomputed radiance transfer. *ACM Trans. Graph.* 22, 3 (2003), 382–391.

SLOAN, P.-P., KAUTZ, J., AND SNYDER, J. Precomputed radiance transfer for real-time rendering in dynamic, low-frequency lighting environments. In *SIGGRAPH '02: Proceedings of the 29th annual conference on Computer graphics and interactive techniques* (New York, NY, USA, 2002), ACM Press, pp. 527–536.

WESTLUND, H. B., AND MEYER, G. W. Applying appearance standards to light reflection models. In *SIGGRAPH '01: Proceedings of the 28th annual conference on Computer graphics and interactive techniques* (New York, NY, USA, 2001), ACM Press, pp. 501–51.

Roman Ďurikovič,
Faculty of Natural Sciences, UCM
Nam. J. Herdu 2, 917 01 Trnava
Slovak Republic
e-mail: roman.durikovic@fmph.uniba.sk

Ivan Šedo
Faculty of Mathematics, Physics and Informatics, Comenius University
Slovak Republic

Received May 2007